https://doi.org/10.48048/tis.2024.8032

Green Synthesis of Silver Nanoparticles using *Moringa oleifera*: Implementation to Photoantimicrobial of *Candida albicans* with LED Light

Imelda Imelda[1], Sri Dewi Astuty[2,*], Paulus Lobo Gareso[2], Zaraswati Dwyana[3], Nur Fadhillah Arifin[4] and Suryani Dyah Astuti[5]

[1]*Magister Program of Physics, Faculty of Mathematics and Natural Sciences, Hasanuddin University, Makassar 90245, Indonesia*
[2]*Departement of Physics, Faculty of Mathematics and Natural Sciences, Hasanuddin University, Makassar 90245, Indonesia*
[3]*Departement of Biology, Faculty of Mathematics and Natural Sciences, Hasanuddin University, Makassar 90245, Indonesia*
[4]*Teeth and Mouth Hospitals, Muslim Indonesia University, Makassar 90122, Indonesia*
[5]*Departement of Physics, Faculty of Science and Technology, Airlangga University, Surabaya 60115, Indonesia*

([*]Corresponding author's e-mail: dewiastuti@fmipa.unhas.ac.id)

Received: 2 February 2024, Revised: 19 February 2024, Accepted: 26 February 2024, Published: 1 July 2024

Abstract

Green synthesis of silver nanoparticles using *Moringa oleifera* (AgNPs/MO) was carried out to produce nanoscale antifungal agents which are used as photosensitizing agents in photoantimicrobial therapy. This study focused on investigating the potential of AgNPs/MO producing some toxic radical compounds that inhibit the growth of *Candida albicans* biofilms. The inhibition mechanism uses the principle of photoinactivation treatment which combines a photosensitizer with an LED light source at a power of 100 mW for 60 - 300 s of exposure. Quantitative data analyzed were the number of viable cells and radical compounds, formed by *malondialdehyde* (MDA) level. It is investigated through staining the XTT (2,3-Bis-(2-Methoxy-4-Nitro-5-Sulfophenyl)-2H-Tetrazolium-5-Carboxanilide) and TBARS (Thiobarbituric Acid Reactive Substances). The results show that the maximum wavelength of AgNPs is 440 nm while the *Moringa oleifera* has 2 peaks at 425 and 635 nm. The maximum effect occurred in the group of photosensitizer AgNPs/MO combined LED with percentage inactivation about 76.80 % for blue LEDs and 76.20 % for red LEDs. The group of LED irradiation without photosensitizer obtained about 51.85 % for blue LEDs and 50.04 % for red LEDs. The MDA level group of AgNPs/MO combined LED also produced MDA levels of 1.772 nmol/mL for blue LED and 1.617 nmol/mL for red LED. Meanwhile, the application of photoantimicrobial using only LEDs produced MDA levels of only 1.353 nmol/mL for blue LEDs and 1.347 nmol/mL for red LEDs. This research has shown that the green synthesis of AgNPs/MO has a good potential to inhibit the growth of *Candida albicans* biofilms as a photosensitizer agent.

Keywords: Photoantimicrobial, Green synthesis, Silver nanoparticles, *Moringa oleifera*, *Candida albicans* biofilms, LED light

Introduction

Infections triggered by pathogenic microbes, including the fungus *Candida albicans* (*Candida albicans*), severely threaten human health [1]. It is known as the most common pathogen that causes infections of the oral and vaginal mucosa, which accounts for 90 % of candidiasis cases [2,3]. The fungus *Candida albicans* can form a more rigid and thick biofilm due to the presence of β-glucan, which is antimicrobial-resistant [4]. Biofilm is a microbial community of cells attached to a tissue/substrate surface covered by an extracellular polymeric substance (EPS) matrix that leaves persistent cells. Cells from *Candida* biofilms can detach and spread throughout the host and invade new sites of infection [5]. Long-term conventional treatment with antibiotics can result in potential health risks, such as drug resistance [6]. Therefore, photoantimicrobial were developed as alternative light-based treatments that can penetrate transparent materials such as biofilms and prevent the emergence of resistance.

Photodynamic therapy (PDT), also known as photoantimicrobial mechanism [7], is an alternative mechanism for dealing with biofilms. A therapeutic system that utilizes the activation of photosensitizer (PS) by light at certain wavelengths. Together with oxygen, it produces various reactive oxygen species, such as singlet oxygen, which is very toxic. This cytotoxic product interacts with cell components, especially proteins, membrane lipids and nucleic acids, causing permanent damage to microorganism cells and even death. According to the Jablonski diagram, the photoantimicrobial mechanism involves 3 activity processes: Photophysical, photochemical and photobiological processes. Photophysical activity consists of the absorption of light energy at certain wavelengths, which causes the excitation of PS* molecules from the lowest energy level to the excitation level ($S_0 \rightarrow S_1$) or ($S_0 \rightarrow S_2$). PS* molecules can return to the ground state (E_0) after experiencing vibrational relaxation and internal conversion down to the singlet ground level ($S_{1,0}$) and emit fluorescence. Another possibility, PS* can undergo conversion to the triplet excitation energy level ($S_1 \rightarrow T$) and carry out a chemical reaction with oxygen molecules to form ROS compounds. PS molecules that are stable at the triplet level return to their ground state by releasing energy in the form of phosphorescence emissions. The release of energy at the triplet level is carried out by PS molecules in 2 ways: Electron transfer to form radical compounds and energy transfer to form singlet oxygen [5,8,9]. Mechanism of photoantimicrobial shown in **Figure 1**.

Some research that applies PDT development can be carried out through PS engineering, ranging from synthetic agents, crude extracts, to green nanoparticle synthesis. Research in the field of nanotechnology plays an active role in the field of modern science and technology. Improved material properties through nanoscale size provide better functionality [10]. Nanomaterials can penetrate a variety of microbial mechanisms, including direct damage to cell walls and membranes [11]. These metal-based nanoparticles interact with cell membranes, thereby disrupting the electron transport chain, permeability and respiratory function of cells. These nanoparticles also destroy bacterial DNA and proteins with the release of metal ions and the formation of reactive oxygen species (ROS) [12-14]. Photoantimicrobial mechanism against *Candida albicans* biofilms which are damaged, especially in the cell walls of the lipid layer and produce malondialdehyde compounds as shown in **Figure 1**.

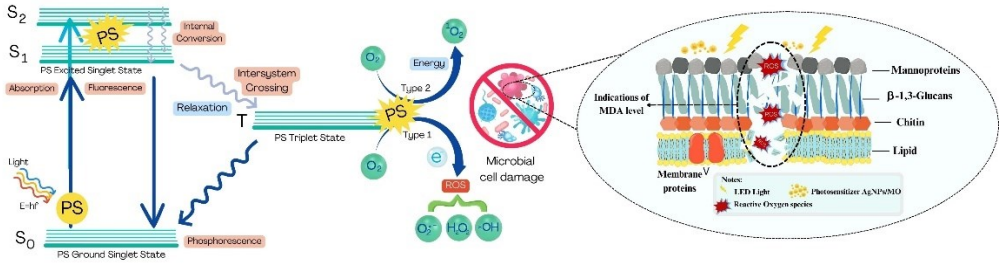

Figure 1 Modified photoantimicrobial system adapted from [51].

Photoantimicrobial system that consists of 3 processes: Photophysical process (absorption and excitation), photochemical process (chemical reaction to produce a radical compound) and photobiological process (toxicity of target cells by ROS which causes cell damage or bacterial death). The mechanism of each process involves attracting PS electron molecules to transition to the triplet level and then interacting with oxygen molecules around the target. Photochemistry causes the production of radical compounds through complex chemical reactions such as ROS which are reactive and very toxic, thus initiating cell death. The photobiological process is the occurrence of cell damage to the cell wall and other cell organelles. The process of microbial cell damage (**Figure 1**) due to attack by ROS compounds, especially on cell walls that contain lipids. Disruption of the lipid structure in the cell wall is called lipid peroxidation, namely damage to the structure and function of the cell membrane which will then oxidize proteins and damage nucleic acids (DNA). Rapidly reactive cell organelles such as DNA, cell membranes and nucleic acids will disrupt cell genetic function and cause cell death [51].

Ag metal or Ag ions are used in various treatments for dental materials, water treatment, textile fabrics, sunscreen lotions, burn wound treatment, etc. This material has high thermal stability and little toxicity to human cells [15-17]. Ag is considered to have effective antifungal, antimicrobial and anticancer effects against various nanoscale pathogens [18]. Currently, nanoparticle production is developed through 3 methods: Chemical, physical and "green" routes, which involve the use of biological reducing agents, including plant extracts and microbial filtrates. The first 2 methods, namely chemical and physical, are often expensive and produce toxic by-products, but the green nano synthesis method has been recognized as a cheap and environmentally friendly process. For these reasons, interest in green synthetic metal nanoparticles is increasing [16,19]. Astuti *et al.* [20] research on antifungal agents using silver nanoparticles activated by a diode laser light source succeeded in reducing around 64.48 ± 0.07 % of *Candida albicans* biofilm [20] .

Moringa oleifera (MO) [21,22] is a plant that is often used in traditional medicine systems. MO acts as a circulatory and cardiac stimulant. MO is an excellent source of flavonoids, phenolic acids, methionine, antioxidant vitamins, cysteine, tocopherol, calcium, β-carotene, potassium, alkaloids, saponins, tannin, steroids metabolite and protein [23,24]. Research conducted by Bindhu *et al.* [25] proved that MO flowers are capable of producing silver nanoparticles which are quite stable in solution. The silver nanoparticles formed show considerable antimicrobial activity compared to other antibiotics so the green synthesis of silver nanoparticles using MO has been proven to be a potential candidate for medical applications [25].

The wavelength of light in the photoantimicrobial mechanism is a very important component in the production of ROS, where the light provided must be safe for host cells (humans). LEDs are light sources that originate from a semiconductor voltage, causing charge injection and light emission. LEDs are cheap, small, flexible and lightweight. The emission wavelengths of available LEDs cover the majority of PS, so LEDs can be selected to match the PS absorption and used without filters [26,27]. Santos *et al.* [28]

conducted research on the application of response surface methodology to evaluate photodynamic inactivation mediated by Eosin Y and 530 nm LEDs against *Staphylococcus aureus* bacteria. Huang *et al*. [1] conducted research on the irradiation of halogen/nitrogen-doped graphene polymer quantum dot LEDs triggering photodynamic inactivation of bacteria in infected wounds. An ideal light source should provide high output power at the wavelengths required for PS activation. Some research says the intensity of the light source that is suitable for photoantimicrobial in fungi is in the range of 10 to 100 mW/cm^2 [29,30].

Research related to photoantimicrobial has reported significant success when using organic PSs such as methylene blue, malachite green, toluidine blue O, 5-ALA and synthetic AgNPs. Other research relies on medicinal plant extracts that produce chlorophyll, curcumin and pheophytin as natural photosensitizing agents. The combination of the potential of medicinal plant extracts with the synthesis of nano silver through green synthesis has also been widely reported as an inhibitor of the growth of microorganisms but not much research has been developed that applies green synthesis as a PS in killing pathogenic microbes. This research combines the synthesis of AgNPs with MO leaf plant extract which aims to optimize the potential of natural ingredients with nanoparticle materials so as to further increase the effectiveness of photoantimicrobial mechanisms. The microbial test sample used in this research is *Candida albicans* biofilm and the light source for illumination was red and blue LEDs.

Materials and methods

Material

Candida albicans cell cultures were obtained from the Indonesian Muslim University's labotatory collection (South Sulawesi, Indonesia). Silver Nitrate ($AgNO_3$) from Sigma-Aldrich Chemical Pvt. Ltd. *Moringa oleifera* (MO) leaf extract is used as a reducing agent in green synthesis. XTT (2.3-Bis-(2-Methoxy-4-Nitro-5-Sulfophenyl)-2H-Tetrazolium-5-Carboxanilide) formation salt 1 mg/mL as a cell viability dye. Menadion 10 mg/mL. Trichloroacetic acid (TCA) 20 % and Thiobarbituric Acid (TBA) 0.67 % from Merck as a TBARS dye for testing Malondialdehyde (MDA) levels. Red LEDs (620 nm) and blue LEDs (450 nm) light source based on a microcontroller system was used in this research.

Research method

This research method starts from preparing green synthesis AgNPs/MO extraction, preparing *Candida Albicans* biofilm, characterization of AgNPs/MO (UV-Vis spectrum test, FTIR and clear zone test), then the samples are given photoantimicrobial treatment based on treatment groups (PS combined LED or LED only), The next stage is to test the success of the photoantimicrobial treatment based on cell viability test using the XTT assay staining and the value of MDA levels through the TBARS staining test.

The extraction of AgNPs/MO

AgNPs/MO is a photosensitizer agent applied to the photoantimicrobial mechanism in this research. This material is formed from a green synthesis process, $AgNO_3$ was reduced using MO extract to become AgNPs which are shown in **Figures 2(a)** and **2(b)**. About 150 g of MO leaves were macerated with 750 mL of methanol:petroleum ether (3:7; v/v) solvent. Maceration was carried out in dark conditions or the bottle was covered with aluminum foil for 2×24 h. Next, it was partitioned with diethyl ether:petroleum ether solvent to separate carotene pigments from chlorophyll pigments.

To prepare the green synthesis of AgNPs/MO, about 0.017 g of Silver Nitrate ($AgNO_3$) powder was dissolved in 100 mL of distilled water to make a 1 mM $AgNO_3$ solution [31]. A total of 10 mL MO chlorophyll extract was added to 90 mL $AgNO_3$ solution until the color of the solution changed from clear

to reddish brown. The indication of the formation color change in the $AgNO_3$ solution to reddish brown color indicates the formation of AgNPs/MO [32].

Biofilm Candida albicans preparation

To prepare the biofilm, one of *Candida albicans* culture that has been rejuvenated is diluted in 10 mL of BHI-B media then vortexed and incubated for 24 h to form inocula. The harvested inocula was placed in an Eppendorf and then centrifuged at 4 °C, 10.000 rpm for 15 min until pellets were formed. Next, the pellets were dissolved in sterile PBS to measure their turbidity with an OD value of 0.729 (detection λ transmission = 600 nm) or the equivalent of 0.5 Mc. Farland. About 500 µL aliquots of *Candida albicans* were planted in Eppendorf tubes and then incubated for 90 min. After that, the tubes were washed with sterile PBS to remove cells that weren't attached to the tube wall. Added 500 µL of BHI-B glucose 8 % then incubated for 48 h to get the optimum biofilm before testing. After that, the sample's fluid were removed, leaving a biofilm attached to the tube wall. The oxygen was flowed into the Eppendorf well for 30 s for each sample, then stored for 15 min in a closed chamber to increase the chance of a reaction between compound radicals, or ROS and molecules of oxygen during the irradiation process. Then 500 µL of PS AgNPs/MO was added to the tube and incubated at 37 °C for 60 min to maximize the potency of PS. The illustration of the biofilm preparation before the photoantimicrobial mechanism is shown in **Figure 2(c)**.

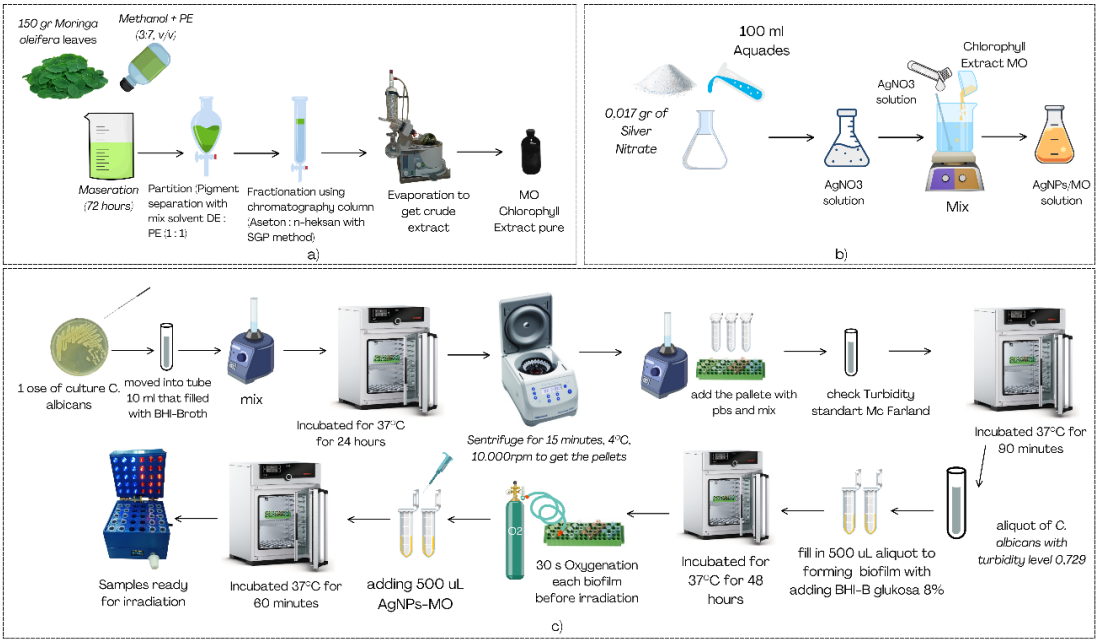

Figure 2 Stage of preparation: (a) MO chlorofil extract, (b) green synthesis of AgNPs/MO as a PS and (c) *Candida albicans* biofilm.

Characterization of AgNPs/MO

UV-Vis spectral analysis

The UV-Vis spectrum test was used to characterize the green synthesis results of AgNPs/MO using a UV-Vis spectrophotometer in the wavelength range 300 - 700 nm. The spectrum observation is used to measure the maximum absorption of AgNPs/MO in the wave length range. This absorbance value is used to determine the percentage of intensity that can be absorbed by AgNPs/MO.

FTIR (Fourier Transform Infrared) spectroscopy analysis

FTIR used to analyze the function groups of the green synthesis results of AgNPs/MO. The characterization of the FTIR shows the silver nanoparticles spectrum of the $AgNO_3$ synthetic result that reacts with the extract of *Moringa oleifera*. This characteristic reveals the bond of any compound contained in the PS [33]. This FTIR analysis is tested in the range 400 to 4,000 cm^{-1}.

Photoantimicrobial procedure

The LEDs instrument of irradiation in this research uses a time variation of 1 to 5 min of irradiation using 100 mW power with a 3 cm distance from the sample to the LEDs light. This instrument is shown in **Figure 3(a)**.

Before the sample was irradiated, 500 µL of AgNPs/MO was added to the wells and incubated for 60 min. The procedure of the irradiation process on the photoantimicrobial as shown in **Figure 3(b)**.

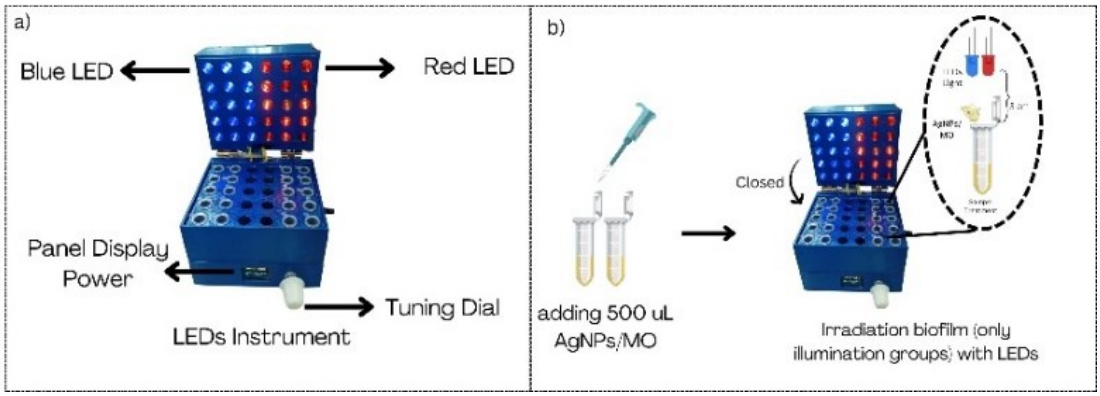

Figure 3 Photoantimicrobial procedure: (a) the LEDs instrument and (b) the process of irradiation.

The function of the tuning dial (**Figure 3**) is to adjust the power output and time that we set on the instrument. The panel display shows the value of the power output and time variation. During the process of irradiation, the cover of the instrument was closed to prevent another light source from entering the room. This irradiation process produces energy that is absorbed by PS which produce radical compounds that can damage the cells. The energy that was absorbed from the LEDs was calculated by using equations:

$$I_{LED} = \frac{P}{A} \quad (1)$$

$$I_{absorbed} = \%(\text{Absorbance}) \times I_{LED} \quad (2)$$

$$E = I_{absorbed} \times t \quad (3)$$

With "%(Absorbance)" is the percentage of photon absorbs of AgNPs/MO at wavelength of 450 and 620 nm according to the LED specification of LED light used in this research. "$I_{absorbed}$" is LED Intensity absorbed by AgNPs/MO (unit: W/cm^2) suitable for each wavelength. "I_{LED}" is the Intensity of each LED which was measured using a luxmeter (unit: W/cm^2). Other symbols: "P" is the output power of the light source (unit: W), "t" is the irradiation time (unit: s). "A" is the beam area of the light source (unit: cm^2), and "E" is the energy of the flux light (J/cm^2) [30,34,35]. The design of treatment groups in this research is shown in **Table 1**.

Table 1 Design of treatment groups.

No.	Group treatment	Description
1	$C_{(-)}$	Control negative (Biofilm)
2	$C_{(+)AgNO3}$	Control positive (Biofilm + $AgNO_3$)
3	$C_{(+)\ MO}$	Control positive (Biofilm + extract chlorophyll MO)
4	$C_{(+)AgNPs/MO}$	Control positive (Biofilm + AgNPs/MO)
5	L_{1M} - L_{5M}	Treatment photoantimicrobial without PS (biofilm + red LEDs) with variation time irradiation 1, 2, 3, 4 and 5 min
6	PL_{1M} - PL_{5M}	Treatment photoantimicrobial with PS (biofilm + AgNPs/MO + red LEDs) with variation time irradiation 1, 2, 3, 4 and 5 min
7	L_{1B} - L_{5B}	Treatment photoantimicrobial without PS (biofilm + blue LEDs) with variation time irradiation 1, 2, 3, 4 and 5 min
8	PL_{1B} - PL_{5B}	Treatment photoantimicrobial with PS (biofilm + AgNPs/MO + blue LEDs) with variation time irradiation 1, 2, 3, 4 and 5 min

Antimicrobial activity test

The test of antimicrobial activity was performed using a disc method that produced a clear zone around *Candida albicans* cell culture by immersing 4 paper discs in a row with $AgNO_3$, AgNPs/MO, MO extract and aquadest. Then paper discs are placed on petri dish containing nutrient media that the biofilm *Candida albicans* has been applied and incubated for 24 h. The diameter of the clear zone that occurs around the paper disc was measured and observed to prove the existence of antimicrobial activity [48].

Cell viability test with XTT assay

XTT assay test aims to detect whether the cell is viable. The coloring process is carried out by adding 100 µL XTT, 1 mg/mL, 5 µL Menadion 10 mg/mL and 395 µL sterile PBS into the Eppendorf tube that contains the sample after photoantimicrobial treatment and then incubating in the oven at a temperature of 37 °C for 2 h. Absorbance was read by using an ELISA reader at 490 nm wavelength. Then, to determine the inactivation value, the following formula is used:

$$\%\ \text{inactivation} = \left|\frac{\text{ODcontrol} - \text{ODtreatment}}{\text{ODcontrol}}\right| \times 100\ \% \quad (4)$$

Optical density (OD) serves as an indicator of cell viability with a yellow to orange gradation color. The more concentrated the color, the more active the cells are in metabolizing and reacting to XTT. The term OD refers to the density of microbial matter determined by the brightness of the sample and absorbance value.

Test MDA levels with the TBARS staining method

The Malondialdehyde level test (MDA) is intended to detect how many radical compounds have accumulated in a tissue. MDA is a compound that forms when a cell reacts with a radical, resulting in cell oxidation. After passing through the irrigation process, the biofilm is cleaned with sterile PBS, added to 1 mL of aquadest, homogenized with vortex and then inserted into the centrifuge at a temperature of 4 °C at a speed of 10.000 rpm for 15 min. After that, biofilm was heated in waterbath at a temperature of 95 °C for 15 min and then stored at room temperature for 1 h. The absorbance at λ_{532nm} was read using the UV-Vis

spectrophotometer. The resulting color of the sample was pink, an indicator of the number of microbes that died after releasing the MDA compound. The following MDA levels were converted using the concentration of TEP (1,1,3,3-tetraethoxypropane) as the compounds of MDA. Determination of MDA level using the following equation:

$$y = ax + b \quad (5)$$

$$\text{MDA level } \left(\frac{\text{nmol}}{\text{mL}}\right) = \frac{y - b}{a} \quad (6)$$

Eq. (5) is a linearity function of the standard curve created based on the TEP concentration which produces the constant values "a" and "b" which are needed to further calculate the MDA content of the sample. From the linearity function, the following value is obtained: a = 0.6373 and b = −0.7972 (the data not shown), then this constant will be substituted in Eq. (6). "y" is the value of absorbance and "x" represents the MDA level.

Statistical analysis

This experiment was replicated 3 times, and the results were presented as the mean ± SD, so we used a statistical test by 1-way ANOVA with significance for ($p < 0.05$) to know each treatment group has a different effect in this mechanism.

Results and discussion

The energy of LED light

Power output from red and blue LEDs was set at 100 mW power for 3,600 s. The mean value of output power of the red LED was measured at 100.24 mW while the mean output power of 99.98 mW for the blue LED. It can be said that the red and blue LEDs used during the radiation were still working well. The energy of red and blue LEDs during irradiation is the result of the light intensity absorbed by AgNPs/MO per irradiation area for a certain duration of time. The results can be seen in the **Table 2**.

Table 2 Data of energy density in photoantimicrobial applicated (absorbance from AgNPs/MO activated with red LED (620 nm) is 0.223 and blue LED (450 nm) is 2.123, irradiation area = 0.785 cm^2.

Energy level	LEDs intensity (W/cm^2)		LEDs intensity absorbed by AgNPs/MO (W/cm^2)		Time (s)	Energy (J/cm^2)	
	Red LED	Blue LED	Red LED	Blue LED		Red LED	Blue LED
E_1					60	3.06	7.56
E_2					120	6.12	15.12
E_3	0.128	0.127	0.051	0.126	180	9.18	22.68
E_4					240	12.24	30.24
E_5					300	15.30	37.80

Table 2 shows the data of energy density from LEDs light to the surface of biofilm *Candida albicans* in the eppendorf well by varying the irradiation time produces different light energy values. The calculations show that the energy density from 100.24 mW of red LEDs is 3.06 J/cm^2 per minute, while the

energy density from 99.98 mW of blue LEDs is 7.56 J/cm^2 per minute. We can see that the 300 s irradiation time of red LED and blue LED produces energy densities of 15.30 and 37.80 J/cm^2, respectively. The longer irradiation time we use in this research produces a higher energy density. Blue LED also shows a higher energy density than red LED because the absorbance of blue LED is higher than that of red LED.

Green synthesis silver nanoparticles using *Moringa oleifera*

The process of green synthesis AgNPs/MO can be observed by changes of color in the solution $AgNO_3$ that has been reduced to AgNPs, as shown in **Figure 4**. The visualization of the color change from yellow to dark brown. These results are similar to the studies by Azarbani and Shiravand [36]. Another observation that can be obtained from this green synthesis process is that the longer the solution AgNPs/MO stay at room temperature, the color of the solution became more concentrated [36-38].

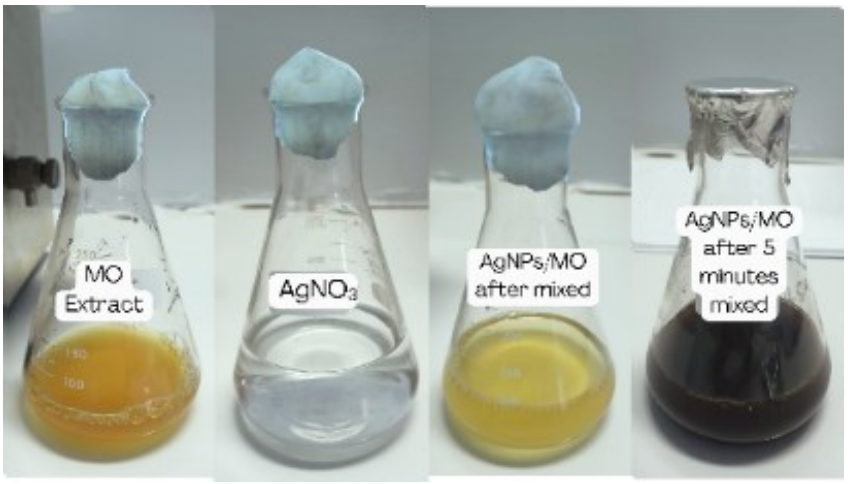

Figure 4 Color visualization of green synthesis AgNPs/MO.

Characterization of PS AgNPs/MO

UV-Vis visible spectra analysis

Characteristics of PS green synthesis AgNPs using *Moringa oleifera* was carried out using a UV-Vis spectrophotometer. This test shows the absorbance of the fotosensitizer in the spectrum range 300 - 700 nm that can be seen in **Figure 5**.

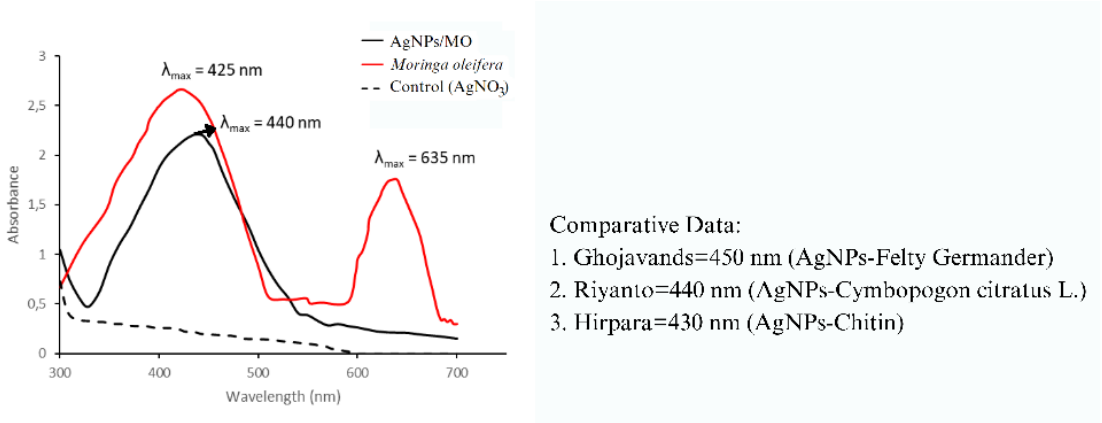

Figure 5 Optimum wavelength of AgNPs/MO, MO extract and $AgNO_3$.

Figure 5 shows the absorption rate of $AgNO_3$, MO extract and AgNPs/MO at wavelengths with a visible light spectrum range of 300 - 700 nm. The absorption rate of the MO extract has 2 peaks. The first peak is λ_1 425 nm with maximum absorbance 2.695 and at the second peak is λ_2 635 nm with maximum absorbance 1.754. The peak UV-Vis absorption spectrum for green synthesis AgNPs/MO is at a wavelength of 440 nm with a maximum absorbance of 2.214. Similar research about optimum wavelength of AGNPs by Riyanto *et al.* [40] obtained wavelengths 440 nm, Ghojavands 450 nm and Hirpara 430 nm. Other studies have noted that the absorption of AgNPs is in the wavelength range 420 - 450 nm [39-42].

Fourier transform infrared spectroscopy

FTIR is used to identify function groups on AgNPs surfaces synthesized using Moringa oleifera leaf extract. This function group is responsible for reducing Ag^+ to Ag^0 [43]. The spectrum of AgNPs/MO shown in **Figure 6**.

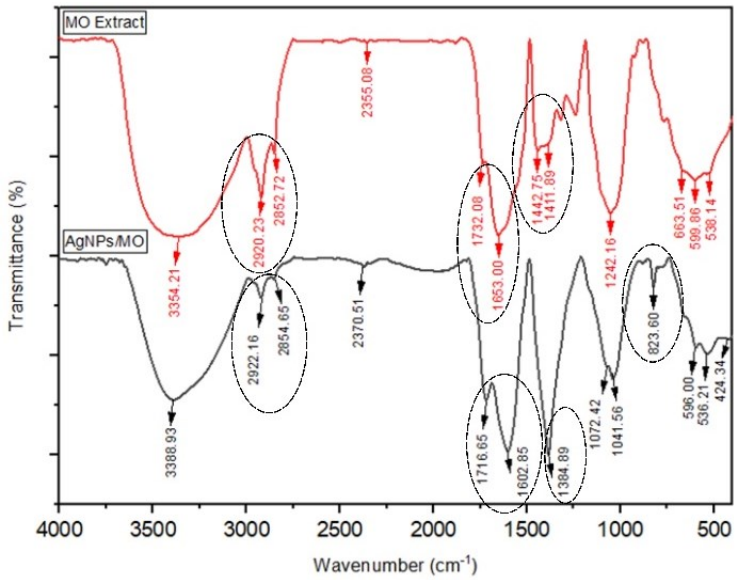

Figure 6 FTIR spectrum of MO Extract and AgNPs/MO.

AgNPs/MO peaks appearing at 424.34, 536.21, 596.00, 823.60, 1,041.56, 1,072.42, 1,384.89, 1,602.85, 1,716.65, 2,061.90, 2,370.51, 2,854.65, 2,922.16 and 3,388.93. Phenolic O-H bonds are seen at 424.34, 536.21 and 596.00. The bonds that appear below 700 cm^{-1} are related to the extract-vibration of the Ag metal. The peak formation of AgNPs occurred at 823.60 cm^{-1}. Peaks 1,041.56 and 1,072.42 refer to the C-O carboxyl group or C-N group which is an extension of the amide bond in the protein. This indicates that MO contains protein. The peak at 1,384.89 cm^{-1} is associated with the symmetric C-H stretching of the alkane groups. The peak at 1,602.85 refers to C=C stretching. The peak at 1,716.65 cm^{-1} is caused by C=O stretching. Peaks 2,854.65 and 2,922.16 refer to strong bonds of the C-H base group. The peak at 2,370.51 cm^{-1} refers to the C≡N nitrile bond. While peak 3,388.93 indicates N-H/O-H binding of phenolic compounds. The presence of phenols and proteins in MO not only serves as a reduction factor but can also act as a stabilizing factor. The leaf of MO contains phenols, carboxylic acids, proteins and terpenoids, which are responsible for the synthesis and reduction of AgNPs [38,45-47].

FTIR test results show a comparison between the MO spectrum (before reducing $AgNO_3$) and the AgNPs/MO spectrum (after green synthesis). Specifically, several transmission peaks can be identified, for

the MO FTIR spectrum it has a wider band, especially in the range 2,700 - 3,500 cm^{-1}. Meanwhile, for the AgNPs/MO spectrum, the peak appears to be single with a transmission value of 60 %. Another identification area, namely in the range 1,200 - 1,700 cm^{-1}, appears to have several insignificant or noise peaks in the spectrum which is different from the FTIR spectrum of AgNPs/MO where single and sharp peaks are seen. This indicates that $AgNO_3$ has the potential to be reduced by MO and can be used as a photosensitizing agent in the photoantimicrobial mechanism of *Candida albicans* biofilms. If we look at the comparison between the characteristics of the AgNPs/MO spectrum based on the profiles displayed in UV-Vis and FTIR, it can be estimated that the appearance of 1 AgNPs/MO peak in the UV-Vis spectrum profile is in line with the many single peaks in the FTIR spectrum profile. Single peaks indicate that the molecule strongly absorbs light at a certain wavelength. Illumination treatment that uses 2 different wavelengths, namely red and blue, still has the potential to be absorbed by AgNPs/MO.

Inhibition of *Candida albicans* biofilm in photoantimicrobial

The disc method was used to conduct antimicrobial activity, which resulted in a clear area surrounding the cell of *Candida albicans*. The circles forming around the disc indicating antifungal activity that inhibited the formation of *Candida albicans* colonies. The diameter of clear zone formed around the AgNPs/MO PS compared to the clear zone formed surrounding the $AgNO_3$ solution, and MO extract are 15.6, 10.5 and 9.7 mm, respectively (the data not shown). It indicates that AgNPs/MO PS have greater antifungal activity than the other 2. Another similar research by Jain and Mehata [48] shows that AgNPs with plant extract (Tulsi extract) have higher antibacterial activities than $AgNO_3$ solution. The clear zone of AgNPs with Tulsi extract is 14 mm, while the $AgNO_3$ solution is only 10 mm.

Cell viability testing using XTT assay staining produces various visualizations of orange degradation ranging from bright to cloudy as seen in **Figure 7**.

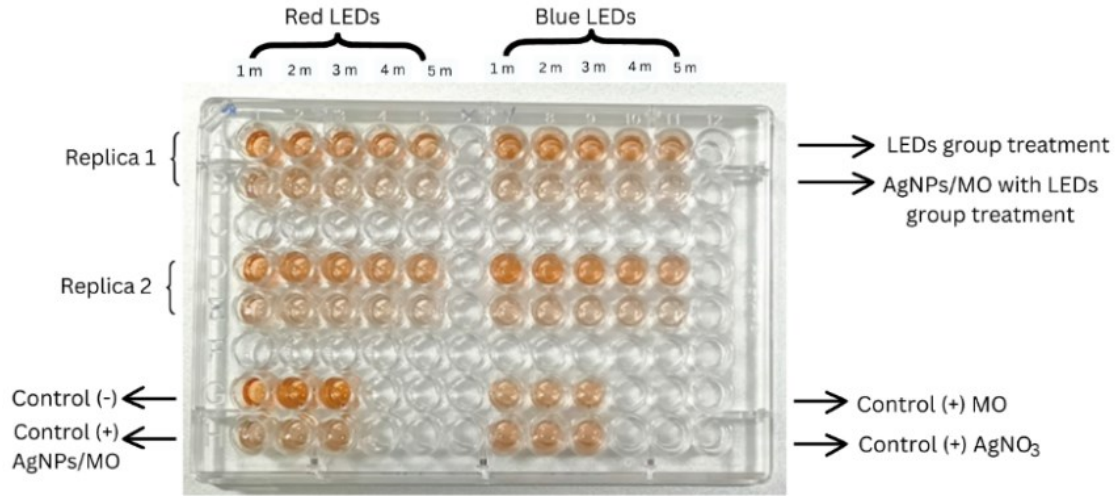

Figure 7 The different color gradation of viability cells using the XTT assay.

The color gradation from yellow to orange that is relevant to the number of viable cells. The color of light orange indicates many cells are still actively metabolized and product dehydrogenase enzymes bind to formasan salt. The data quantitative of OD is presented in **Figure 8**.

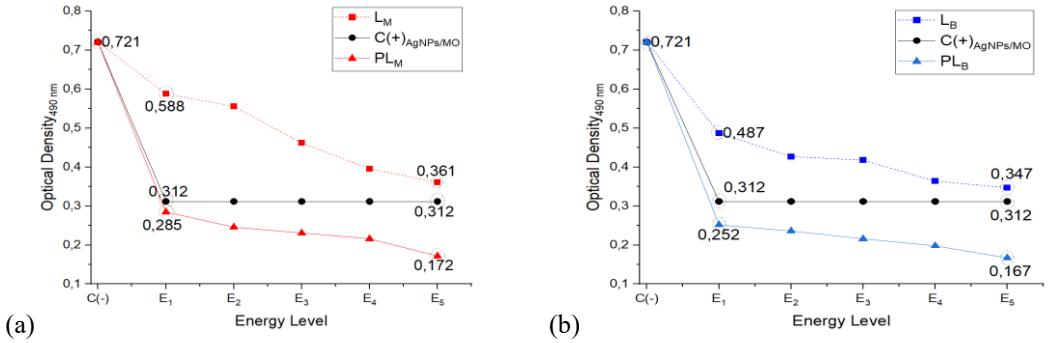

(a) (b)

Figure 8 The optical density (OD) value reduction curve for *Candida albicans* biofilm resulting from photoantimicrobial treatment using radiation: (a) red LED and (b) blue LED.

Figure 8 shows a decreasing trend in optical density values depending on the energy level of the 2 types of LEDs used. Each graph displays 3 curves, each representing the positive control group (only AgNPs/MO). The PS LED without treatment group (L_M and L_B), and the combined PS with LED treatment group (PL_M and PL_B). The starting point of the OD value for group C(–) is a reference for reduction from the other 3 treatment groups. For the positive control group, the OD value decreased from 0.721 ± 0.004 to 0.312 ± 0.004. **Figure 8(a)** shows the result of photoantimicrobial using red LED only, which has decreased the OD value from 0.721 ± 0.004 to 0.361 ± 0.001 and the photoantimicrobial using PS combined with red LED has decreased the effective OD value from 0.721 ± 0.004 to 0.172 ± 0.002. **Figure 8(b)** shows that the photoantimicrobial using only blue LED could reduce the OD value from 0.721 ± 0.004 to 0.347 ± 0.002. The smallest reduction in OD values occurred in the combination group of PS and blue LED. It went from 0.721 ± 0.004 to 0.167 ± 0.002. The PL_{5B} group is significantly different at ($p < 0.05$) compared to the other groups. The lowest OD value occurs at a higher energy level, namely E_5, with an irradiation time of 5 min. Because it has less viability, it is the most optimal treatment in this research. Biofilms irradiated with blue LEDs also had lower viability values than the group irradiated with red LEDs. This is probably because AgNPs/MO absorption properties are more optimal in the blue spectrum, which has implications for many AgNPs molecules that have the opportunity to produce ROS compounds. Another suggestion is that the blue spectrum wavelength (450 - 495 nm) has a higher energy so that the existence of AgNPs/MO after being excited is relatively longer at the triplet level. This opportunity has a strong synergy with the number of dead microbes.

Further analysis was carried out to determine the percentage of inactivation for each treatment using Eq. (6). The percentage of inactivation results is presented in **Figure 9**.

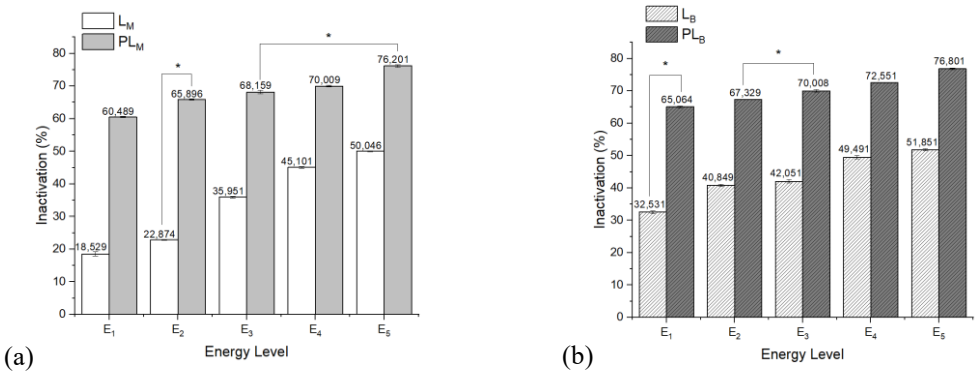

(a) (b)

Figure 9 The inactivation percentage of treatment group by (a) blue LEDs and (b) red LEDs.

Figure 9 shows the statistics of the 1-way ANOVA test with lines connecting data that is significantly different between treatments at the confidence level ($p < 0.05$). The statistical test results for all treatments were significantly different. The images shown with connecting lines in the 2 radiation groups are representative for all data including the significance between groups of radiation treatments with and without PS as well as between treatment groups with different energy levels.

Figure 9(a) shows Red LEDs group (L_M) inactivated the *Candida albicans* about (18.529 ± 0.607 to 50.046 ± 0.175) % from 1 to 5 min of irradiation. While the group of PS combined with Red LEDs (PL_{5M}) could inactivate this microbe higher than the other, it is about (60.489 ± 0.182 to 76.201 ± 0.376) % from 1 to 5 min of irradiation. **Figure 9(b)** shows that blue LEDs groups with PS or not (L_B and PL_B) are more effective than red LEDs groups with PS or not (L_M and PL_M). The inactivation percentage of L_B groups from 1 to 5 min of irradiation is about (32.531 ± 0.332 to 51.851 ± 0.309) %. The group of PS with blue LEDs could inactivate this microbe from (65.064 ± 0.273 to 76.801 ± 0.322) % during the irradiation process, so we can say that the PS combined with blue LEDs is a great photoantimicrobial agent compared to the other groups in this research. It is because the energy density of blue LED is higher than the energy density of Red LED. This study is in line with research conducted by Toan *et al*. [49] that showed blue LED has reduced 90 % *S.aureus* and 60 % *E. coli* with an energy dose of 230.10 J/cm^2. Several studies related to photoantimicrobial using AgNPs. Singh and Mohanlall [50] examined the activity of *Cassia occidentalis* biocatalyst with Silver Nanoparticles, AgNPs showed a 70.90 % inhibitory potential at 1,000 µg/mL against some gram-positive and gram-negative bacteria. Astuty *et al.* [34] also studied the effectiveness of lasers using AgNPs photosensitizer with Jatrohpa leaf chlorophyll and succeeded in reducing *Candida albicans* biofilms to 60 - 80 % using a 650 nm laser.

The test for Malondialdehyde levels (MDA) is designed to measure the quantity of radical compounds that have built up in a tissue. The increasing amount of MDA formed indicates the increasing number of ROS compounds produced. Assuming that every single ROS compound will damage 1 cell, the higher the MDA level, the more successful the photoantimicrobial results. The color produced on the sample is pink, which is an indicator of how many microbes die after releasing the MDA compound. The amount of MDA formed is analyzed as the number of radical compounds or singlet oxygen formed during photoantimicrobial treatment. The higher the number of microbial deaths, the greater the intensity of the brightness of the pink color, the more it tends to be purple. The color gradation from MDA levels can be shown in **Figure 10**. This figure shows the differences in solution color in each treatment group. The pink color indicates the presence of more MDA compounds. MDA is a metabolite product after lipid peroxidation occurs in the Candida albicans cell wall due to attack by ROS compounds produced during the photoantimicrobial mechanism. This principle is based on the assumption that 1 microbe releases 1 MDA compound because it is attacked by 1 ROS compound.

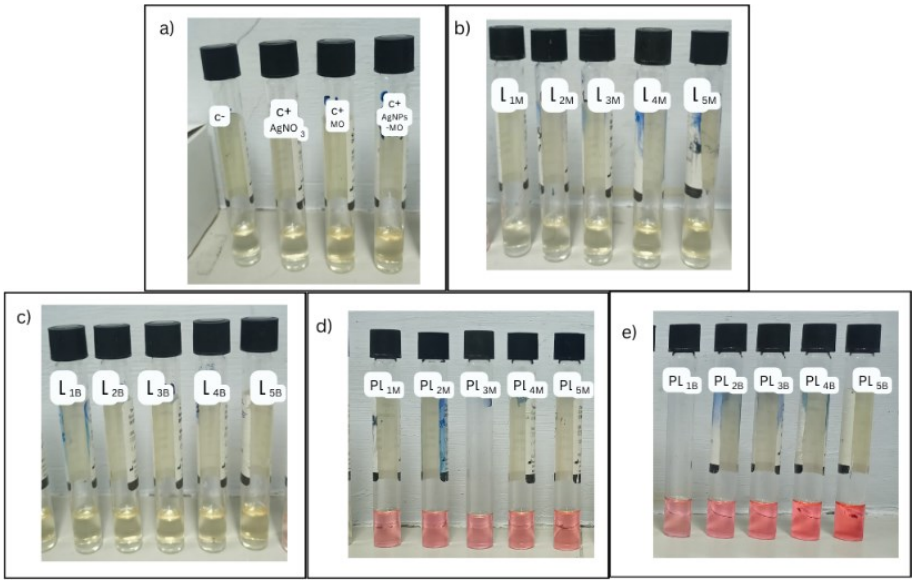

Figure 10 The different levels of MDA shown by color gradation: (a) control group, (b) treatment group using red LED, (c) treatment group using blue LED, (d) treatment group using PS combined with red LED and (e) treatment group using PS combined with blue LED.

The quantitative OD value of MDA can be shown at **Figure 11**.

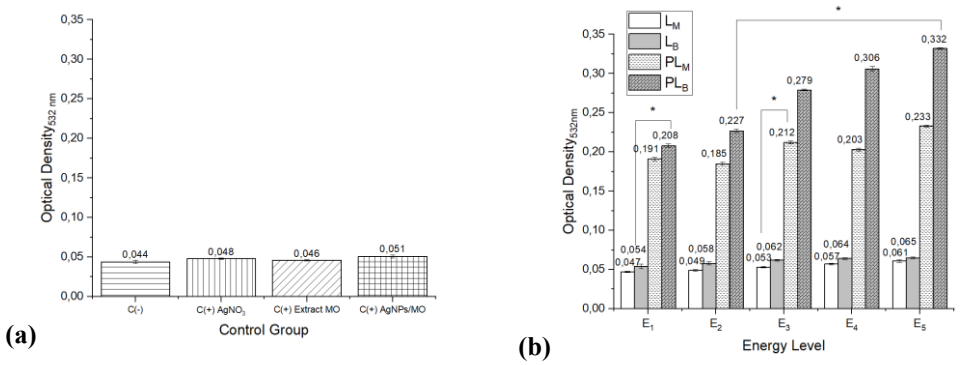

Figure 11 The absorbance at OD_{532nm}: (a) control group and (b) treatment group ($p < 0.05$).

Figure 11 shows the statistics of the 1-way ANOVA test with lines connecting data that are significantly different between treatments at the confidence level ($p < 0.05$). **Figure 11(a)** shows the statistical test results from the control group are not significantly different. While the data statistical test results in **Figure 11(b**) for the treatments group were significantly different ($p < 0.05$). The images show that there are connecting lines in the 2 radiation groups, namely L_B and PL_B in the first energy level, L_M and PL_M in the third energy level, and the other data PL_{2B} and PL_{5B} represent significant difference in the data ($p < 0.05$) based on their energy levels. The more irradiation time we use and the more energy absorbed by PS, the more cell death occurs. **Figure 11(a)** showed that the highest OD_{532nm} was in the AgNPs/MO control group (0.051 ± 0.001) compared to other control groups. $AgNO_3$ control group (0.046 ± 0.001) and MO extract (0.048 ± 0.001). This is because the more Malondialdehyde compounds are formed, the more ROS compounds are produced, causing more cells to be damaged. This shows that PS combined with or

without LED irradiation has the potential to inhibit the growth of *Candida albicans* biofilms, even though the amounts are relatively small. Meanwhile, **Figure 11(b)** shows the OD_{532nm} value for the photoantimicrobial treatment group of PS with blue LEDs for the length of irradiation of 300 s (PL_{5B}) is (0.332 ± 0.001). The PS with red LEDs group obtains an OD (PL_{5M}) of (0.233 ± 0.001). PS combined with LED light has a higher OD than treatment group PS without LED. The OD_{532nm} for blue LEDs only (L_{5B}) in 5 min of irradiation is (0.065 ± 0.002). This value is higher than the red LEDs (L_{5M}) that is only about (0.061 ± 0.002). It can be said that the use of PS combined with LED light is also more effective than the samples that only use irradiation only or PS only. The use of AgNPs/MO PSs with blue LEDs also produces a *Malondialdehyde* compound that causes more cell death than red LEDs. MDA compounds are products of lipid peroxidation from every pathogenic microbe, especially *Candida albicans*, which has thicker lipid cell wall components. The more lipid peroxidation occurs, the higher the degree of MDA level produced and correlated with the number of dead cells. The TBA reagent binds several MDA compounds using a TCA reagent catalyst. This oxidative stress marker is widely used to measure metabolic enzymes, mitochondrial function and cell metabolism.

Furthermore, the MDA level is determined using the absorption value read at λ_{532nm} in Eq. (6). The MDA level value is shown in **Figure 12**.

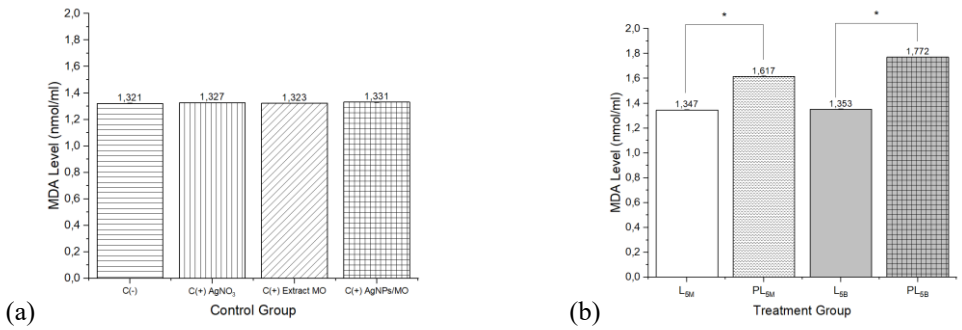

Figure 12 MDA level: (a) control group and (b) treatment group. This data is statistically significant at $p < 0.05$.

Figure 12(a) shows the MDA value resulting from the control group. The MDA level of the control group (−) is 1.321 nmol/mL. It is lower than the other positive controls, $AgNO_3$, extract MO and AgNPs/MO are 1.327, 1.323 and 1.331 nmol/mL, respectively. Meanwhile, in **Figure 12(b)**, the mean value of the MDA using AgNPs/MO treatment irradiated with red LEDs is 1.617 ± 0.002 nmol/mL and higher for blue LEDs is 1.772 ± 0.002 nmol/mL. The samples that were only irradiated with a red LED without a PS had MDA levels of around 1.347 ± 0.003 nmol/mL and for blue LEDs around 1.353 ± 0.001 nmol/mL. So, it can be said that the value of MDA levels in samples that went through the photoantimicrobial process with LED irradiation and using a PS were very good when compared to samples without using a PS. Blue LEDs is also have higher MDA levels than red LEDs.

Comparable research was conducted by Astuty *et al.* [29] using laser light with the addition of papaya leaf chlorophyll produces the malondialdehyde levels of 0.467 and 0.397 nmol/mL for 650 and 445 nm laser, respectively. Statistical tests between the control (+) and (−) groups were not significantly different. But there is significantly different value ($p < 0.05$) of MDA level between the treatment group of LEDs only and the PS with LEDs combination group, as seen in **Figure 12**. It demonstrates that this photoantimicrobial mechanism treatment has more potential when a combination of light and PS is applied

to kill microbial cells. It also shows that the blue LED treatment group has a higher value compared to the Red LED treatment group. It is because the blue LED absorbs more energy than the red LED.

The application of green synthesis AgNPs/MO as a photosensitizer in photoantimicrobial mechanism to inhibit microbe pathogens. This is useful in the medical and pharmaceutical fields to eradicate infectious diseases. It is hoped that in the future this photosensitizer can be applied in more diverse forms such as cream, gel or liquid so that it can be easily applied above the wound. Further, AgNPs/MO is not only used as antibacterial agents but they can also be applied as conductive nanofluids, bio-sensors, catalysis, water treatment, etc.

Conclusions

Implementation of photoantimicrobial applications using photosensitizer from green synthesis of AgNPs/MO with LED light has been proven to have the potential to inhibit the growth of *Candida albicans* biofilms. The use of Moringa oleifera as a natural reductant for green synthesizers is very well demonstrated by the maximum wavelength of AgNPs is 440 nm while the Moringa oleifera has 2 peaks at 425 and 635 nm. The maximum effect occurred in the group of photosensitizer AgNPs/MO combined LED with percentage inactivation about 76.80 % for blue LEDs and 76.20 % for red LEDs. The group of LED irradiation without photosensitizer obtained about 51.85 % for blue LEDs and 50.04 % for red LEDs. The MDA level group of AgNPs/MO combined LED also produced MDA levels of 1.772 nmol/mL for blue LED and 1.617 nmol/mL for red LED. Meanwhile, the application of photoantimicrobial using only LEDs produced MDA levels of only 1.353 nmol/mL for blue LEDs and 1.347 nmol/mL for red LEDs. This research has shown that the green synthesis of AgNPs/MO has a good potential to inhibit the growth of *Candida albicans* biofilms as a photosensitizer agent. The different OD and MDA values of each treatment group showed that AgNPs/MO has great potential as photosensitizers in photoantimicrobial systems. The group of photosensitizers combined with light was more effective than the light treatment group alone, and the use of blue light was more optimal than red light.

Acknowledgements

The authors of this paper thank LP2M Hasanuddin University, Indonesia for funding this research as a part of Grant Penelitian Fundamental Kolaborasi (PFK) 2023 with contract No. 000323/UN4.22/PT.01.03/2023.

References

[1] HH Huang, A Anand, CJ Lin, HJ Lin, YW Lin, SG Harroun and CC Huang. LED irradiation of halogen/nitrogen-doped polymeric graphene quantum dots triggers the photodynamic inactivation of bacteria in infected wounds. *Carbon* 2021; **174**, 710-22.

[2] PJS Maia, I de Aguiar, M dos Santos Velloso, D Zhang, ER dos Santos, JR de Oliveira, JC Junqueira, M Selke and RM Carlos. Singlet oxygen production by a polypyridine ruthenium (II) complex with a perylene monoimide derivative: A strategy for photodynamic inactivation of *Candida albicans*. *J. Photochem. Photobiol. A Chem.* 2018; **353**, 536-45.

[3] RA Fristiyanti, NS Matin, SD Ratnaningrum, N Nurdiana, S Santoso and RD Hanifarizani. Efficacy comparison of oral and intravaginal *Lactobacillus plantarum* administration on Secreted Aspartyl Protease-5 (SAP5) levels in Vulvovaginal candidiasis. *Trends Sci*. 2023; **21**, 7225.

[4] M Henriques and S Silva. *Candida albicans* virulence factors and its pathogenicity. *Microorganisms* 2021; **9**, 704.

[5] JC Carmello, F Alves, FG Basso, CA de Souza Costa, AC Tedesco, FL Primo, EGO Mima and AC Pavarina. Antimicrobial photodynamic therapy reduces adhesion capacity and biofilm formation of *Candida albicans* from induced oral candidiasis in mice. *Photodiagnosis Photodynamic Ther.* 2019; **27**, 402-7.

[6] JMA Blair, MA Webber, AJ Baylay, DO Ogbolu and LJV Piddock. Molecular mechanisms of antibiotic resistance. *Nat. Rev. Microbiol.* 2015; **13**, 42-51.

[7] CN Lin, SJ Ding and CC Chen. Synergistic photoantimicrobial chemotherapy of methylene blue-encapsulated chitosan on biofilm-contaminated titanium. *Pharmaceuticals* 2021; **14**, 346.

[8] I Yoon, JZ Li and YK Shim. Advance in photosensitizers and light delivery for photodynamic therapy. *Clin. Endosc.* 2013; **46**, 7-23.

[9] SD Astuty and A Baktir. The effectiveness of laser diode induction to *Carica Papaya L.* chlorophyll extract to be ROS generating in the photodynamic inactivation mechanisms for *C.albicans* biofilms. *J. Phys. Conf. Ser.* 2017; **853**, 012026.

[10] AE Nel, L Mädler, D Velegol, T Xia, EMV Hoek, P Somasundaran, F Klaessig, V Castranova and M Thompson. Understanding biophysicochemical interactions at the nano-bio interface. *Nat. Mater.* 2009; **8**, 543-57.

[11] Y Wang, Y Jin, W Chen, J Wang, H Chen, L Sun, X Li, J Ji, Q Yu, L Shen and B Wang. Construction of nanomaterials with targeting phototherapy properties to inhibit resistant bacteria and biofilm infections. *Chem. Eng. J.* 2019; **358**, 74-90.

[12] S Stankic, S Suman, F Haque and J Vidic. Pure and multi metal oxide nanoparticles: Synthesis, antibacterial and cytotoxic properties. *J. Nanobiotechnol.* 2016; **14**, 73.

[13] TC Dakal, A Kumar, RS Majumdar and V Yadav. Mechanistic basis of antimicrobial actions of silver nanoparticles. *Front. Microbiol.* 2016; **7**, 1831.

[14] Y Abo-zeid and GR Williams. The potential anti-infective applications of metal oxide nanoparticles: A systematic review. *Wiley Interdiscipl. Rev.* 2020; **12**, e1592.

[15] RA Raj, MS AlSalhi and S Devanesan. Microwave-assisted synthesis of nickel oxide nanoparticles using *Coriandrum sativum* leaf extract and their structural-magnetic catalytic properties. *Materials* 2017; **10**, 460.

[16] S Devanesan, MS AlSalhi, RV Balaji, AJA Ranjitsingh, A Ahamed, AA Alfuraydi, FY AlQahtani, FS Aleanizy and AH Othman. Antimicrobial and cytotoxicity effects of synthesized silver nanoparticles from *Punica granatum* peel extract. *Nanoscale Res. Lett.* 2018; **13**, 315.

[17] RA Fernandes, AA Berretta, EC Torres, AFM Buszinski, GL Fernandes, CC Mendes-Gouvêa, FND Souza-Neto, LF Gorup, ERD Camargo and DB Barbosa. Antimicrobial potential and cytotoxicity of silver nanoparticles phytosynthesized by pomegranate peel extract. *Antibiotics* 2018; **7**, 51.

[18] M Lalunio-Manikan, AP Bonto and CMH Ebreo. Nanosilver immobilized in carbonaceous particles derived from hydrothermal carbonization of *Eleusine indica* leaf extract. *Trends Sci.* 2021; **18**, 681.

[19] KH Min, JW Shin, MR Ki and SP Pack. Green synthesis of silver nanoparticles on biosilica diatomite: Well-dispersed particle formation and reusability. *Process Biochem.* 2023; **125**, 232-8.

[20] SD Astuti, PS Puspita, AP Putra, AH Zaidan, MZ Fahmi, A Syahrom and Suhariningsih. The antifungal agent of silver nanoparticles activated by diode laser as light source to reduce *C. albicans* biofilms: An *in vitro* study. *Laser. Med. Sci.* 2019; **34**, 929-37.

[21] A Pareek, M Pant, MM Gupta, P Kashania, Y Ratan, V Jain, A Pareek and AA Chuturgoon. *Moringa oleifera*: An updated comprehensive review of its pharmacological activities, ethnomedicinal,

phytopharmaceutical formulation, clinical, phytochemical, and toxicological aspects. *Int. J. Mol. Sci.* 2023; **24**, 2098.

[22] N Kumar, Pratibha and S Pareek. *Bioactive compounds of Moringa (Moringa species). In*: HN Murthy and KY Paek (Eds.). Bioactive compounds in underutilized vegetables and legumes. Springer, Cham, Switzerland, 2021.

[23] PMP Ferreira, DF Farias, JTDA Oliveira and ADFU Carvalho. *Moringa oleifera*: Bioactive compounds and nutritional potential. *Revista de Nutricao* 2008; **21**, 431-7.

[24] RA Syahputra, R Fajrina, Z Rani and A Rahmadani. Producing polyurethane as wound plaster using glycerol transesterified of waste cooking oil with Moringa leaf extract (*Moringa Oleifera Lam.*) as an antimicrobial. *Trends Sci.* 2023; **20**, 6963.

[25] MR Bindhu, M Umadevi, GA Esmail, NA Al-Dhabi and MV Arasu. Green synthesis and characterization of silver nanoparticles from *Moringa oleifera* flower and assessment of antimicrobial and sensing properties. *J. Photochem. Photobiol. B* 2020; **205**, 111836.

[26] M Piksa, C Lian, IC Samuel, KJ Pawlik, IDW Samuel and K Matczyszyn. The role of the light source in antimicrobial photodynamic therapy. *Chem. Soc. Rev.* 2023; **52**, 1697-722.

[27] EM Setiawatie, SD Astuti and AH Zaidan. An *in vitro* anti-microbial photodynamic therapy (aPDT) with blue LEDs to activate chlorophylls of Alfalfa Medicago sativa L on aggregatibacter actinomycetemcomitans. *J. Int. Dent. Med. Res.* 2016; **9**, 118-25.

[28] AR Santos, AFD Silva, AFP Batista, CF Freitas, E Bona, MJ Sereia, W Caetano, N Hioka and JMG Mikcha. Application of response surface methodology to evaluate photodynamic inactivation mediated by Eosin Y and 530 nm LED AGAINST staphylococcus aureus. *Antibiotics* 2020; **9**, 125.

[29] SD Astuty, Suhariningsih, A Baktir and SD Astuti. The efficacy of photodynamic inactivation of the diode laser in inactivation of the *Candida albicans* biofilms with exogenous photosensitizer of papaya leaf chlorophyll. *J. Laser. Med. Sci.* 2019; **10**, 215-24.

[30] TN Mileto and FG Azambuja. Low-intensity laser efficacy in postoperative extraction of third molars. *RGO Revista Gaúcha de Odontologia* 2017; **65**, 13-9.

[31] I Laib, BD Ali and O Boudebia. Green synthesis of silver nanoparticles using *Helianthemum lippii* extracts (Hl-NPs): Characterization, antioxidant and antibacterial activities and study of interaction with DNA. *J. Organomet. Chem.* 2023; **986**, 122619.

[32] JS Moodley, SBN Krishna, K Pillay, Sershen and P Govender. Green synthesis of silver nanoparticles from *Moringa oleifera* leaf extracts and its antimicrobial potential. *Adv. Nat. Sci. Nanosci. Nanotechnol.* 2018; **9**, 015011.

[33] S Patel and N Patel. *Tectona grandis* seed mediated green synthesis of silver nanoparticles and their antibacterial activity. *Trends Sci.* 2023; **20**, 5104.

[34] SD Astuty, Y Handayani, R Abdullah, S Hajar and PM Tabaika. Mediated sensitizer of nanosilver-chlorophyll Jatropha leaf. *Indonesian Phys. Rev.* 2023; **6**, 132-45.

[35] M Zain, SD Astuty, S Dewang, B Armynah, RR Wahyudi and S Ramadhana. Analysis of the changes power output and energy dose to green laser against OD and MDA values after photoinactivation at *Candida Albicans* and *Staphyloccocus epidermidis* associate biofilms. *AIP Conf. Proc.* 2023; **2719**, 020006.

[36] F Azarbani and S Shiravand. Green synthesis of silver nanoparticles by *Ferulago macrocarpa* flowers extract and their antibacterial, antifungal and toxic effects. *Green Chem. Lett. Rev.* 2020; **13**, 41-9.

[37] S Ryu, SH Nam and JS Baek. Green synthesis of silver nanoparticles (AgNPs) of *Angelica Gigas* fabricated by hot-melt extrusion technology for enhanced antifungal effects. *Materials* 2022; **15**, 7231.

[38] M Younas, MH Rasool, M Khurshid, A Khan, MZ Nawaz, I Ahmad and MN Lakhan. *Moringa oleifera* leaf extract mediated green synthesis of silver nanoparticles and their antibacterial effect against selected gram-negative strains. *Biochem. Syst. Ecol.* 2023; **107**, 104605.

[39] S Ghojavand, M Madani and J Karimi. Green synthesis, characterization and antifungal activity of silver nanoparticles using stems and flowers of felty germander. *J. Inorg. Organomet. Polymer. Mater.* 2020; **30**, 2987-97.

[40] Riyanto, M Mulwandari, L Asysyafiiyah, MI Sirajuddin and N Cahyandaru. Direct synthesis of lemongrass (*Cymbopogon citratus L.*) essential oil-silver nanoparticles (EO-AgNPs) as biopesticides and application for lichen inhibition on stones. *Heliyon* 2022; **8**, e09701.

[41] DG Hirpara and HP Gajera. Green synthesis and antifungal mechanism of silver nanoparticles derived from chitin-induced exometabolites of *Trichoderma interfusant*. *Appl. Organomet. Chem.* 2020; **34**, e5407.

[42] ZA Ali, R Yahya, SD Sekaran and R Puteh. Green synthesis of silver nanoparticles using apple extract and its antibacterial properties. *Adv. Mater. Sci. Eng.* 2016; **2016**, 4102196.

[43] AK Nzekekwu and OO Abosede. Green synthesis and characterization of silver nanoparticles using leaves extracts of neem (*Azadirachta indica*) and bitter leaf (*Vernonia amygdalina*). *J. Appl. Sci. Environ. Manag.* 2019; **23**, 695.

[44] M Mohammadi, SA Shahisaraee, A Tavajjohi, N Pournoori, S Muhammadnejad, SR Mohammadi, R Poursalehi and HH Delavari. Green synthesis of silver nanoparticles using *Zingiber officinale* and *Thymus vulgaris* extracts: Characterisation, cell cytotoxicity and its antifungal activity against *Candida albicans* in comparison to fluconazole. *IET Nanobiotechnology* 2019; **13**, 114-9.

[45] S Sampaio and JC Viana. Production of silver nanoparticles by green synthesis using artichoke (*Cynara scolymus L.*) aqueous extract and measurement of their electrical conductivity. *Adv. Nat. Sci. Nanosci. Nanotechnology* 2018; **9**, 045002.

[46] GM Mohammed and SN Hawar. Green biosynthesis of silver nanoparticles from *Moringa oleifera* leaves and its antimicrobial and cytotoxicity activities. *Int. J. Biomater.* 2022; **2022**, 4136641.

[47] N Pal, M Agarwal and A Ghosh. Green synthesis of silver nanoparticles using polysaccharide-based guar gum. *Mater. Today Proc.* 2023; **76**, 212-8.

[48] S Jain and MS Mehata. Medicinal plant leaf extract and pure flavonoid mediated green synthesis of silver nanoparticles and their enhanced antibacterial property. *Sci. Rep.* 2017; **7**, 15867.

[49] LC Toan, LX Nghiem, TQ Toan, PT Thi and H Chi. Design panel of hexagonal nanowire-based blue LEDs for inactivation bacteria in food safety. *J. Austrian Soc. Agr. Econ.* 2022; **18**, 1259-67.

[50] S Singh and V Mohanlall. Biocatalytic and biological activities of *Cassia occidentalis* mediated silver nanoparticles. *Trends Sci.* 2022; **19**, 1712.

[51] X Wang, D Luo and JP Basilio. Photodynamic therapy: Targeting cancer biomarkers for the treatment of cancers. *Cancers* 2021; **13**, 2992.